

## STRUCTURAL AND MAGNETIC PROPERTIES, AND MAGNETIC DOMAIN STRUCTURE IN ULTRASOFT $\text{Fe}_{73.5-x}\text{Cr}_x\text{Nb}_3\text{Cu}_1\text{Si}_{13.5}\text{B}_9$ MAGNETIC ALLOYS

Andrés Rosales<sup>1</sup>, Víctor Hugo Valencia, Jorge A. Morales, Abilo Andrés Velásquez  
*Universidad Nacional de Colombia, Sede Manizales*

### ABSTRACT

The structural and magnetic properties of  $\text{Fe}_{73.5-x}\text{Cr}_x\text{Nb}_3\text{Cu}_1\text{Si}_{13.5}\text{B}_9$  alloy ribbons have been studied after appropriate processing achieving nanocrystalline structure and showing ultrasoft magnetic behavior, especially giant magnetoimpedance effect, GMI[1]. Characterization has been performed by X-ray diffraction (XRD), vibrating sample magnetometry (VSM), GMI measurements and atomic force microscopy/magnetic force microscopy (AFM/MFM). Particular attention has been paid to observation of domain structure by MFM imaging. A periodic stripe domain structure is generally observed. A comparison between structural and magnetic properties (i.e. coercivity, remanence) and magnetic domain structures of above compounds is presented, and such properties are analyzed in connection with the GMI effect .

### INTRODUCTION

It is now twelve years since the giant magneto-impedance (GMI) effect was observed [2-4]; this effect consists of a large variation of the impedance,  $Z$ , both real and imaginary components of a soft magnetic conductor, when submitted to a relatively small dc magnetic field or a stress. Sensitivity of up 500%/Oe has been observed in the very low field region (less than 1 Oe) field region. In agreement to existing results, to observe GMI, the material has to have good soft magnetic properties (i.e. high permeability and low coercive force), and appropriate domain structure (typically, a transverse one for ribbons in plane, transverse to the ribbon axis and to the applied dc field as well), and a circumferential one for wires. The structural and magnetic properties of the alloy ribbons  $\text{Fe}_{73.5-x}\text{Cr}_x\text{Nb}_3\text{Cu}_1\text{Si}_{13.5}\text{B}_9$  with  $x = 0$  and 10 are studied here by X-ray diffraction (XRD), vibrating sample magnetometry, GMI measurements and atomic force microscopy/magnetic force microscopy (AFM/MFM). A comparison between structural and magnetic properties and magnetic domain structures of above compounds is presented, and such properties are analyzed in connection with GMI effect.

### EXPERIMENTAL DETAILS

The samples structure was analyzed by X-ray diffraction in a D8 Advance Bruker AXS diffractometer using a  $\text{CuK}\alpha_1$  radiation. In addition, a SPM Autoprobe CP (Park Scientific Instruments) was used for investigation of the domain structure. The two-pass technique was used for MFM image, both topography and magnetic were obtained simultaneously.

The spectra were taken at room temperature. The magnetic characteristics such as saturation magnetization  $M_s$ , coercivity  $H_c$ , were measured by a vibrating sample magnetometer for  $H$  up to 10 KOe.

The magneto-impedance ratio with applied magnetic field is defined as [5]:

---

<sup>1</sup> Director of Laboratory of Magnetism: arosales@epm.net.co.

$$\frac{\Delta Z}{Z} = \frac{[Z(H) - Z(H_{Max})]}{Z(H_{Max})} \times 100 \%$$

$Z(H)$  is the impedance measured at the DC field  $H$ .  $Z(H_{Max})$  is the impedance measured at the maximum DC field  $H$  ( $H_{Max} = 75$  Oe). The magneto-impedance was measured by using the so-called four-point method by which a given AC current flows along the magnetic conductor and a voltage is picked up its ends, as is illustrated in block diagram of the figure 1. The measurements were performed at room temperature in the frequency range  $0.1 < f < 12$  MHz.

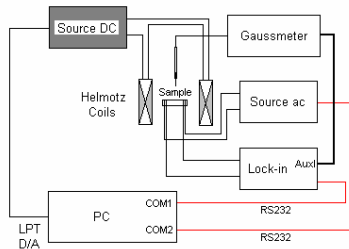


Figure 1. GMI Technique Block Diagram.

RESULTS

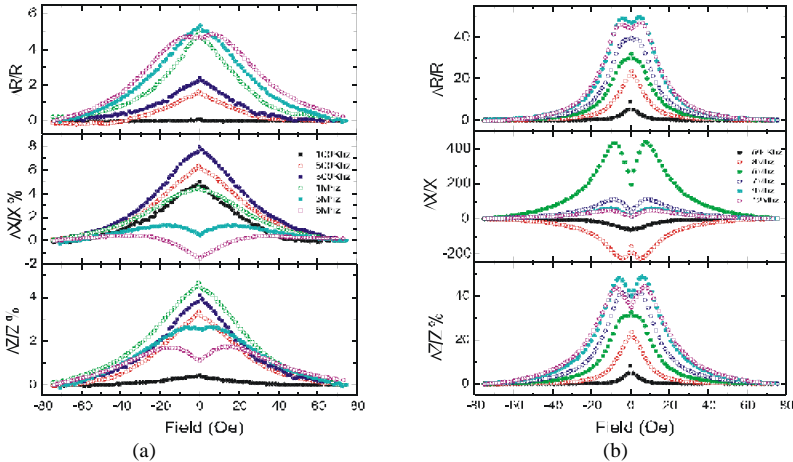


Figure 2.: Reactive,  $\Delta X/X$ , and Resistive  $\Delta R/R$ , components, and total Impedance,  $\Delta Z/Z$  for a ribbon at different frequencies: (a)  $Fe_{73.5}Nb_3Cu_1Si_{13.5}B_9$ . (b)  $Fe_{63.5}Cr_{10}Nb_3Cu_1Si_{13.5}B_9$

For the  $Fe_{73.5}Nb_3Cu_1Si_{13.5}B_9$  alloy ribbon, in the low frequency regime ( $f < 1$  MHz),  $\Delta Z/Z$ , displays a sharp peak at the DC magnetic field  $H = 0$  (single peak behavior). The amplitude of the  $\Delta Z/Z$  increases and the peaks becomes broad but reasonably well defined with increasing frequency. The change of impedance is attributed to the magneto-inductive effect arising

from the transverse magnetization process. Our results in the low frequency regime are in agreement with those previously observed in alloy ribbon nanocrystalline.

For higher frequencies ( $3 < f < 5$  MHz), the  $\Delta Z/Z$  peak splits into two symmetric broad peaks at  $H_+ > 0$  and  $H_- < 0$ , with  $H_+ = H_-$  (two peaks behavior). The amplitude of the  $\Delta Z/Z$  decreases and the position of the broad peaks show a slightly frequency dependence. The results that we obtained in the intermediate frequency regime are in agreement with those previously observed in alloy ribbon nanocrystalline [6]. The  $\Delta Z/Z$  behavior in  $\text{Fe}_{63.5}\text{Cr}_{10}\text{Nb}_3\text{Cu}_1\text{Si}_{13.5}\text{B}_9$  found at the whole frequency interval of measurements is similar to the  $\Delta Z/Z$  behavior observed in  $\text{Fe}_{73.5}\text{Nb}_3\text{Cu}_1\text{Si}_{13.5}\text{B}_9$ , but the frequency limits where single peak regime and two peaks regime are observed in  $\text{Fe}_{63.5}\text{Cr}_{10}\text{Nb}_3\text{Cu}_1\text{Si}_{13.5}\text{B}_9$  are higher than observed ones in  $\text{Fe}_{73.5}\text{Nb}_3\text{Cu}_1\text{Si}_{13.5}\text{B}_9$ .

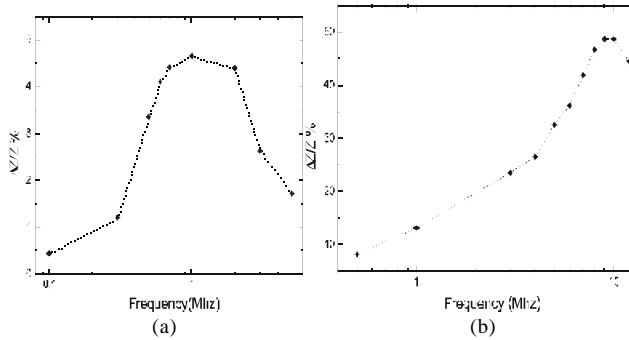


Figure 3.: The frequency dependence of  $\Delta Z/Z$  for: (a)  $\text{Fe}_{73.5}\text{Nb}_3\text{Cu}_1\text{Si}_{13.5}\text{B}_9$ . (b)  $\text{Fe}_{63.5}\text{Cr}_{10}\text{Nb}_3\text{Cu}_1\text{Si}_{13.5}\text{B}_9$ .

For the  $\text{Fe}_{73.5}\text{Nb}_3\text{Cu}_1\text{Si}_{13.5}\text{B}_9$  alloy, in the low frequency regime ( $f < 1$  MHz), The frequency dependence of  $\Delta Z/Z$  for  $\text{Fe}_{73.5}\text{Nb}_3\text{Cu}_1\text{Si}_{13.5}\text{B}_9$ ,  $\Delta Z/Z$  reaches a maximum value ( $\sim 5\%$ ) at frequency of 1Mhz.. For  $f < 2$ Mhz  $\Delta Z/Z$  displays a single peak behavior. For  $f > 2$ Mhz  $\Delta Z/Z$  displays a two peaks behavior ( $H \neq 0$ ). For  $\text{Fe}_{63.5}\text{Cr}_{10}\text{Nb}_3\text{Cu}_1\text{Si}_{13.5}\text{B}_9$ ,  $\Delta Z/Z$  reaches a maximum value ( $\sim 40\%$ ) at frequency of 10Mhz.;  $\Delta Z/Z$   $\text{Fe}_{63.5}\text{Cr}_{10}\text{Nb}_3\text{Cu}_1\text{Si}_{13.5}\text{B}_9$  is higher than  $\Delta Z/Z$  for  $\text{Fe}_{73.5}\text{Nb}_3\text{Cu}_1\text{Si}_{13.5}\text{B}_9$ . This difference in the values  $\Delta Z/Z$  can be mainly attributed to the differences in the electrical resistivities of these alloys [7].

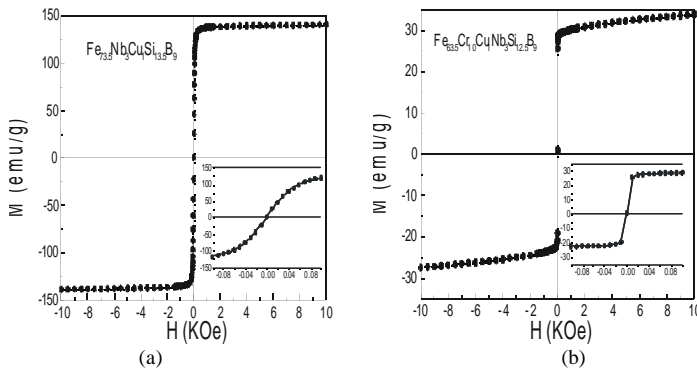


Figure 4. : The hysteresis loops for: (a)  $Fe_{73.5}Nb_3Cu_1Si_{13.5}B_9$ . (b)  $Fe_{63.5}Cr_{10}Nb_3Cu_1Si_{13.5}B_9$ .

The saturation magnetization are: 142 emu/g for  $Fe_{73.5}Nb_3Cu_1Si_{13.5}B_9$ , and 30 emu/g for  $Fe_{63.5}Cr_{10}Nb_3Cu_1Si_{13.5}B_9$  alloy ribbon.

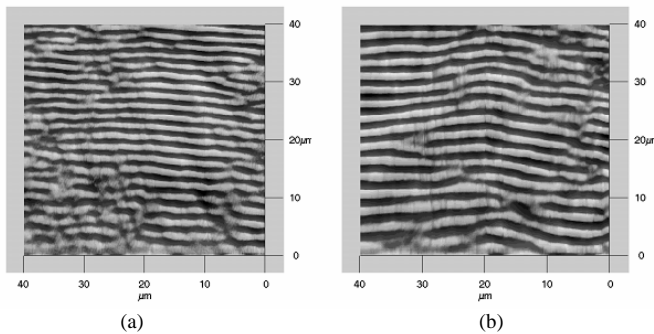


Figure 5.: MFM domain structure. (a)  $Fe_{73.5}Nb_3Cu_1Si_{13.5}B_9$ . (b)  $Fe_{63.5}Cr_{10}Nb_3Cu_1Si_{13.5}B_9$ .

MFM images show a magnetic domain structure reasonably well defined, but the magnetic domain structure of  $Fe_{63.5}Cr_{10}Nb_3Cu_1Si_{13.5}B_9$  is better defined than one observed in  $Fe_{73.5}Nb_3Cu_1Si_{13.5}B_9$ .

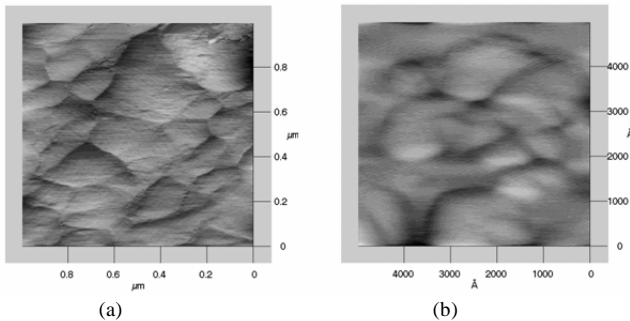


Figure 6.: AFM topography images. (a)  $Fe_{73.5}Nb_3Cu_1Si_{13.5}B_9$ . (b)  $Fe_{63.5}Cr_{10}Nb_3Cu_1Si_{13.5}B_9$ .

The topographic image shows a grain structure reasonably well defined, but the grain structure of  $\text{Fe}_{73.5}\text{Nb}_3\text{Cu}_1\text{Si}_{13.5}\text{B}_9$  is better defined than the observed one for  $\text{Fe}_{63.5}\text{Cr}_{10}\text{Nb}_3\text{Cu}_1\text{Si}_{13.5}\text{B}_9$ . The overall grain size for  $\text{Fe}_{73.5}\text{Nb}_3\text{Cu}_1\text{Si}_{13.5}\text{B}_9$  was  $0.32\ \mu\text{m}$  and it for  $\text{Fe}_{63.5}\text{Cr}_{10}\text{Nb}_3\text{Cu}_1\text{Si}_{13.5}\text{B}_9$  was  $0.18\ \mu\text{m}$ .

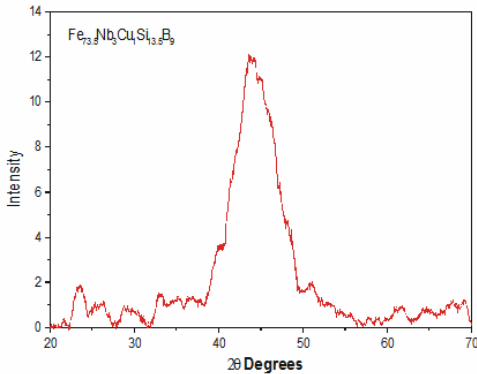


Figure 7.: XRD pattern for  $\text{Fe}_{73.5}\text{Nb}_3\text{Cu}_1\text{Si}_{13.5}\text{B}_9$

The XRD pattern for  $\text{Fe}_{73.5}\text{Nb}_3\text{Cu}_1\text{Si}_{13.5}\text{B}_9$  shows a broad peaks reasonably well defined which resembles the nanocrystalline state in agreement with the grain structure obtained by atomic force microscopy in the same sample.

### CONCLUSION

Based on figures (2a,2b); (3a,3b) (4a,4b), and (5a,5b), we can observed that  $\Delta Z/Z$  of  $\text{Fe}_{63.5}\text{Cr}_{10}\text{Nb}_3\text{Cu}_1\text{Si}_{13.5}\text{B}_9$  is greater than  $\Delta Z/Z$  of  $\text{Fe}_{73.5}\text{Nb}_3\text{Cu}_1\text{Si}_{13.5}\text{B}_9$ , due to the domain structure and the magnetic characteristics of  $\text{Fe}_{63.5}\text{Cr}_{10}\text{Nb}_3\text{Cu}_1\text{Si}_{13.5}\text{B}_9$  are better.

### ACKNOWLEDGMENTS

The authors thank to miss Yulieth Arango, Diego Arias members of the Plasma Group of the UNC manizales branch for the assistance in XRD and MFM measurement, and Dr. M. Coisson of the Instituto Elettrotecnico Nazionale Galileo Ferraris for providing the sample  $\text{Fe}_{73.5}\text{Nb}_3\text{Cu}_1\text{Si}_{13.5}\text{B}_9$ .

### REFERENCES

- [1] Y-F. Li et al., "Giant Magnetoimpedance Effect and Magnetoelastic Properties in Stress-Annealed FeCuNbSiB Nanocrystalline Wire," IEEE Trans. Magnetic., vol. MAG-38, pp. 3096-3098, 2002.
- [2] V.E. Makhotkin, B.P. Shurukhin, V.A. Lopatin, P. Yu. Marchukov, Yu.K. Levin, sensors Actuators A 25-27 (1991) 759.
- [3] F.L.A. Machado, B. Lopes da Silva, E. Montarroyos, J. Appl. Phys. 73 (1993) 687.
- [4] K. Mandal, S.K. Ghatak, Phys. Rev. B 47 (1993) 14233.
- [5] M. Vazquez, J. Magn. Magn. Matter; 226-230 (2001) 693-693.
- [6] H. Chiriac and T.-A. Óvári, IEEE Transactions on Magnetics. Vol. 38 No. 5 3057-3062 (2002).
- [7] M. Knobel, H. Chiriac, J.P. Sinhecker, S. Marinescu, T. A. Óvári, and A. Inohue, Sensors and actuators A: Physical 59 (1997), P. 256].